IIETA International Information and Engineering Technology Association
Advancing the World of Information and Engineering

Annales de Chimie - Science des Matériaux
Vol. 49, No. 4, August, 2025, pp. 375-383
Journal homepage: http://iieta.org/journals/acsm

The Effect of Magnesium Addition to Al-10Si Alloy Through Casting at 740°C on Mechanical Properties: A Simulation Study

Enos Tambing[1], Mickael Ruben Kaiway[1], Samuel Parlindungan Siregar[1], Obet Takke Ranteallo[1], Joni[2*], Eka Irianto Bhiftime[3], Endang Hartiningsih[4]

[1] Department of Mechanical Engineering, Cenderawasih University, Jayapura 99351, Indonesia
[2] Renewable Energy Engineering, Graduate School of Cenderawasih University, Jayapura 99351, Indonesia
[3] Department of Military Mechanical Engineering, Indonesia Defense University, Bogor 16810, Indonesia
[4] Department of Mining Engineering, Cenderawasih University, Jayapura 99351, Indonesia

Corresponding Author Email: joni@ftuncen.ac.id

https://doi.org/10.18280/acsm.490405

Received: 21 June 2025
Revised: 2 August 2025
Accepted: 12 August 2025
Available online: 31 August 2025

Keywords:
Al10SiMg alloys, Mg_2Si precipitation, strength-ductility tradeoff, High Pressure Die Casting, artificial aging, cooling rates

ABSTRACT

Alloys made of Aluminum and silicon (Al-Si) are essential for manufacturing lightweight parts in the automotive and aerospace sectors because of their outstanding ability to be cast and their favorable strength-to-weight ratio. The precise influence of magnesium (Mg) inputs and the various high-pressure die casting (HPDC) variables on their operational success is not entirely comprehended. The examination delves into how the introduction of magnesium in a regulated manner influences the microstructural and mechanical attributes of Al-10Si alloys cast at 740 degrees Celsius. Three compositions were tested: 0 g (0 wt%), 15 g (~3.3 wt%), and 25 g (~5.25 wt%) Mg per 500 g melt, processed via HPDC with dies preheated to 250°C and 7 MPa pressure, followed by T5 heat treatment for aging. The simulations conducted with JMatPro focused on crystallization dynamics, magnesium distribution analysis, Mg_2Si deposition effects, and their respective influence on secondary dendrite arm spacing (SDAS), along with hardness and tensile strength metrics. Moderate Mg additions accelerated Mg_2Si formation, refining the microstructure and significantly increasing hardness and UTS to 420–480 MPa at ~3.3 wt% Mg. Higher Mg levels (~5.25 wt%) further boosted hardness but formed coarser intermetallics, reducing ductility and slightly lowering UTS. These trends align with findings where Mg refines eutectic silicon from strips to fibers, enhancing strength but risking brittleness at higher concentrations.

1. INTRODUCTION

The enthusiasm surrounding Al10Si alloys has considerably grown within materials research, especially when it comes to their implementation in the automotive and aerospace sectors. This particular alloy mixture is quite impressive because of its beneficial strength-to-weight ratio, outstanding castability, and less than ideal thermal expansion coefficient, which makes it fitting for engine parts and structural pieces that are needed to work dependably under combined thermal and mechanical forces [1, 2]. In the automotive domain, the transition towards aluminum-silicon composites is propelled by the persistent necessity for weight reduction to augment fuel efficiency and vehicular efficacy [3]. In aeronautical applications, these alloys are utilized in constituents necessitating elevated strength-to-weight ratios without undermining structural integrity—a pivotal requisite under flight conditions [1, 4].

The infusion of magnesium (Mg) in Al–10Si alloys is imperative for elevating mechanical performance through the establishment of Mg_2Si precipitates, which enhance the material via techniques of precipitation hardening [5]. Introducing magnesium into the Al-10Si mixture boosts hardness and tensile strength, particularly when used with the right heat treatments such as solution treatment and subsequent aging [6, 7]. Solution treatment within the temperature range of 530–570°C (typically around 550°C), followed by rapid quenching, enhances the solid solubility of alloying elements and significantly influences the final hardness and tensile strength after aging [8].

In the realm of scholarly research, it is commonly noted that an Mg concentration nearing 2 wt.% serves as the prime threshold for achieving a balance of strength and ductility in Al–10Si alloys, with tensile strength showing significant enhancements at this formulation [8]. Other investigations document peak ultimate tensile strength (UTS) metrics of approximately 310 MPa and yield strength (YS) nearing 250 MPa under ideal circumstances [9]. However, increasing Mg content beyond this optimum may lead to the formation of coarser Mg_2Si precipitates—reducing ductility (e.g., elongation of approximately 6%) and even decreasing UTS [10]. Furthermore, literature indicates that the strengthening effect of Mg_2Si enables the material to maintain deformation resistance at intermediate service temperatures; for instance, the strain rate at ~100 MPa can be as low as 1×10^{-5} s^{-1} at

~200°C, and Al–10Si–Mg alloys can retain most of their yield strength up to approximately 250°C, although specific values depend on precise conditions and require experimental verification [11, 12].

The ideal Mg concentration for attaining harmonized mechanical characteristics in Al–10Si alloys is roughly 2 wt.%, as documented by Jin et al. [8], who demonstrated significant tensile strength enhancement at this composition, albeit with variations depending on specific processing conditions. While the integration of Mg augments the material characteristics of Al–10Si, appropriate thermal processing is essential to fully exploit the alloy's potentialities. Solution treatment within the 530–570°C temperature range significantly enhances desirable properties. When materials are heated to roughly 550°C and subsequently cooled quickly, it frequently improves the solid solubility of alloying elements, leading to a notable effect on the hardness and tensile strength once aging occurs [8].

Most existing studies are experimental in nature, while research integrating simulation approaches to evaluate the combined effects of Mg content variations and heat treatment strategies remains limited. Emerging computational approaches—such as predictive phase and precipitation kinetics models—facilitate accelerated outcome prediction and alloy design for specific industrial applications, but a cohesive framework for comprehensive composition–treatment interaction analysis is still needed [13, 14]. Thus, two major research gaps are identified: (1) limited systematic studies integrating software-based predictive simulations to map the influence of Mg content variations in Al–10Si under casting conditions at 740°C; and (2) insufficient research directly correlating Mg_2Si phase/precipitation predictions with macroscopic mechanical property predictions (yield strength, ultimate tensile strength, elastic modulus, and hardness) under specific casting process conditions [15, 16].

Based on this foundation, the present study aims to computationally evaluate the estimated changes in macroscopic mechanical properties resulting from compositional variations of Mg additions (0, 15, and 25 g) to Al–10Si alloy under High Pressure Die Casting (HPDC) conditions at 740°C. The research outcomes are expected to generate composition-property maps as preliminary data for further experimentation and design of Mg-modified Al–10Si alloys for industrial applications.

2. MATERIALS AND METHODS

2.1 Alloy compositions

The results of this investigation emphasize the Al-10Si alloy Figure 1 (a) as a crucial material because of its extraordinary variety of attributes, offering significant mechanical strength, high castability, and a low thermal expansion coefficient. This particular alloy system demonstrates remarkable compatibility for sophisticated engineering tasks, notably those that demand extensive production through the High Pressure Die Casting (HPDC) approach, which is the central theme of this research. One significant consideration in creating engine components and ensuring structural integrity for automotive and aerospace industries is the material's lighter density paired with its outstanding strength-to-weight characteristics. The chemical formulation of the Al-10Si alloy employed comprises 10.34 wt.% Si, 0.27 wt.% Mg, and 85.41 wt.% Al, with negligible augmentations of Fe, Cu, and Mn.

a) Al-10Si alloy b) Magnesium pure

Figure 1. Material specimen

To investigate the influence of magnesium (Mg) additions, three distinct compositional variants were prepared by incorporating high-purity Mg Figure 1 (b) into 500 g, 485 g, and 475 g base melts of Al-10Si alloy. These specific Mg addition levels—0 g, 15 g, and 25 g—were deliberately selected to capture a range of its effects on the alloy's properties. The 0 g Mg inclusion functioned as the reference group, furnishing a pivotal benchmark for evaluation. The 15 g Mg addition (approximately 3.26 wt.%) was chosen to examine the effects of an intermediate, and potentially optimal, Mg concentration anticipated to yield maximum precipitation strengthening. Finally, the 25 g Mg addition (approximately 5.25 wt.%) was included to investigate effects beyond the optimal concentration, where the formation of coarser intermetallic compounds is expected to detrimentally affect certain mechanical properties, thereby elucidating a critical strength–ductility trade-off.

2.2 High Pressure Die Casting (HPDC) parameters

The alloy batches were first melted at 690°C to ensure complete homogenization. Following the introduction of Mg into the molten Al–Si system, the melt was mechanically stirred at 90 rpm for 120 seconds to ensure uniform solute distribution. It was thereafter reheated to a casting temperature of 740°C before undergoing processing through the High Pressure Die Casting (HPDC) methodology (Figure 2). This particular casting temperature was chosen to ensure the complete dissolution of all alloying constituents—a fundamental prerequisite for subsequent precipitation hardening. The die underwent preheating to 250°C to alleviate thermal shock, and the casting process was carried out under a consistent pressure of 7 MPa with a die retention period of 6 minutes. Once the substance hardened, the samples were permitted to cool to ambient temperature, given the existing environmental factors. The detailed process parameters are summarized in Table 1.

2.3 Heat treatment

To attain optimal mechanical properties, the cast alloys underwent a T5 heat treatment cycle. The procedure initiated with a solute treatment at 500°C for 60 minutes to dissolve soluble constituents and preserve a supersaturated solid solution. This was immediately followed by rapid water quenching to retain the metastable supersaturated structure. The quenched specimens were subsequently subjected to artificial aging at 150°C for 240 minutes to facilitate the nucleation and growth of strengthening Mg_2Si precipitates. Ultimately, the specimens were subjected to a reduction in temperature to room temperature through stagnant air,

culminating in the ultimate microstructure designated for subsequent examination.

2.4 Simulation workflow

Computational simulations were performed using the JMatPro software to predict the phase equilibrium, solidification behavior, and mechanical performance for each Mg addition level (0, 15, and 25 g). The simulation workflow followed a systematic sequence: equilibrium phase diagram analysis, Scheil solidification modeling to predict solute segregation trends, and construction of solidification and SDAS diagrams to evaluate transformation kinetics. A precipitation model was employed to estimate the evolution of Mg_2Si fraction and particle size. Ultimately, the review of mechanical features—comprising yield strength (YS), ultimate tensile strength (UTS), and hardness—was undertaken concerning the concentration of magnesium and the speed of cooling.

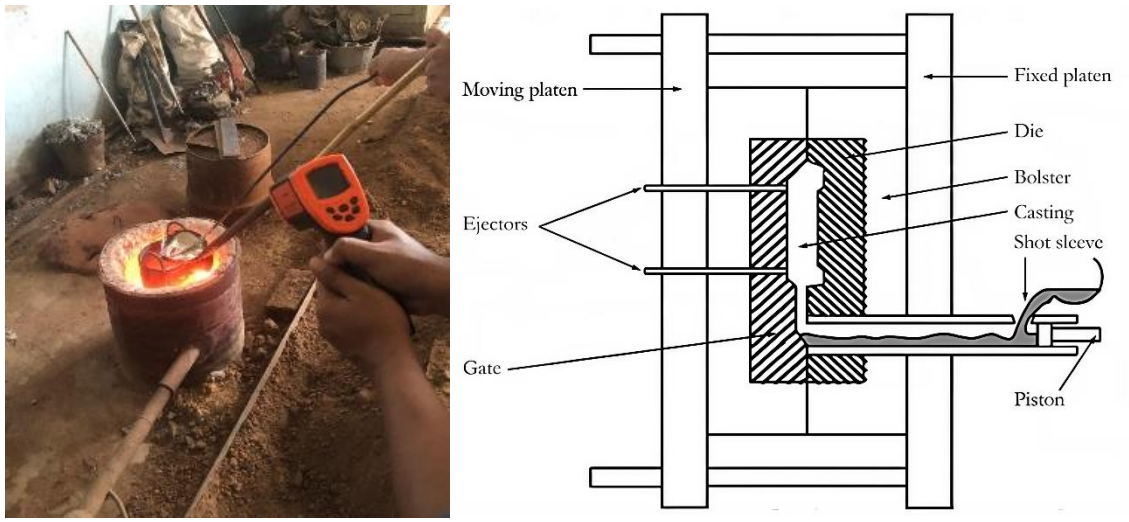

a) Smelting b) HPDC cast

Figure 2. High Pressure Die Casting (HPDC) process

Table 1. Process parameters

Process Step	Value	Unit
Base alloy mass	500; 485; 475	g
Base alloy composition (wt%)	Si 10.34; Mg 0.27; Al 85.41; Fe 0.87; Cu 1.81; Mn 0.16; Others 1.017	wt%
Initial melt temperature	690	℃
Mg addition mass	0; 15; 25	g
Mg composition (wt%)	Si 0.013; Mg 99.93; Al 0.022; Fe 0.003; Cu 0.012; Mn 0.012; Others 0.018	wt%
Mechanical stirring speed	90	rpm
Stirring duration	120	s
Reheat temperature	740	℃
Mold preheats temperature	250	℃
Casting method	HPDC (High Pressure Die Casting)	—
Casting pressure	7	MPa
Mold hold time	6	min
Cooling after casting	Air cooling to room temperature	—
Solution treatment temperature	500	℃
Solution treatment time	60	min
Quench medium	Water	—
Aging temperature	150	℃
Aging time	240	min
Final cooling	Air cooling to room temperature	—

3. RESULT AND DISCUSSION

3.1 Chemical composition and phase solidification

Chemical analysis of the prepared alloys confirmed a systematic shift in composition with incremental additions of pure Mg. As summarised in Table 2, the baseline Al–10Si alloy composition comprised 10.34 wt.% Si, 0.27 wt.% Mg, and 85.41 wt.% Al. The augmentation of 15 g of Mg elevated the Mg concentration to 3.26 wt.%, whilst simultaneously diminishing Al and Si levels to 82.85 wt.% and 10.03 wt.%, respectively. A further addition of 25 g Mg resulted in a Mg content of 5.25 wt.%, with corresponding reductions in Al and Si to 81.14 wt.% and 9.82 wt.%. These systematic compositional changes are attributed to the dilution effect resulting from Mg additions, which progressively reduce the concentration of the base alloy elements.

Simulations of Scheil-type solidification for Al-10Si alloys with progressive Mg additions (0.27, 3.26, and 5.26 wt.%) revealed systematic solute redistribution during solidification (Figure 3). The aluminum content in the remaining liquid displayed a gradual reduction from roughly 86 wt.% at the start of solidification to about 65–70 wt.% as it got closer to being finished. Copper, initially stable, exhibited a gradual increase

followed by a sharp rise to ~25–28 wt.% in the final 5–10% of liquid. Magnesium demonstrated significant segregation, increasing from ~0.3 wt.% in the base alloy to ~6–8 wt.% at 95% solid fraction under low Mg conditions, with further amplification observed in alloys containing 3.26 and 5.26 wt.% Mg. Silicon remained relatively stable at 11-13 wt.%, consistent with its role in Al-Si eutectic formation, while Fe and Mn concentrations remained low but showed tendencies to increase at high solid fractions, suggesting potential formation of Al-Fe-Si intermetallics. These results indicate that increasing nominal Mg content not only enhances Mg segregation but also modifies the partitioning behavior of Cu and Si, ultimately promoting a refined Al-Si-Mg-Cu eutectic microstructure following die casting of high pressure (HPDC).

Table 2. Mixed chemical composition of Al10Si and Mg

Materials	Chemical Composition (%)						
	Si	Mg	Al	Fe	Cu	Mn	Other
Al10Si alloy	10.34	0.27	85.41	0.87	1.81	0.16	1.02
Mg pure	0.013	99.930	0.022	0.003	0.012	0.012	0.018
Al10Si alloy 500g + 0g Mg	10.34	0.27	85.41	0.87	1.81	0.16	1.02
Al10Si alloy 485g + 15g Mg	10.03	3.26	82.85	0.84	1.76	0.16	0.99
Al10Si alloy 475g + 25g Mg	9.82	5.25	81.14	0.83	1.72	0.15	0.97

The scrutinized segregation configurations correspond with recognized Scheil-Gulliver forecasts, wherein solutes exhibiting partition coefficients $k < 1$ are incrementally expelled into the liquid phase throughout solidification. The latest results concerning AlSi10Mg alloys indicate akin enrichment behaviors for Cu, Mg, and Si within the parameters established by Scheil. Van Cauwenbergh et al. [17] reported that solidification of AlSi10Mg at varying cooling rates produced significant interdendritic segregation driven by solute enrichment during advanced solidification stages. Complementary experimental studies on HPDC alloys quantify the cooling rate effect on microstructure: in AlSi9Cu3, secondary dendrite arm spacing (SDAS) decreased approximately 20% as cooling rates increased from 60 to 120 $K \cdot s^{-1}$, while 0.2% proof strength increased from 261 to 335 MPa under equivalent conditions. Hennum et al. [18] further observed that reduced SDAS accelerates β-Mg_2Si precipitation kinetics, thereby enhancing the hardening capacity of Mg-enriched Al-Si alloys.

The results of solute separation, along with fast solidification, bear important significance for the structural integrity and capabilities of alloys [19]. Increased Mg additions (0.27 to 5.26 wt.%) enhance precipitation hardening potential through Mg_2Si precursor enrichment in interdendritic regions, while refined Al-Si eutectics under HPDC conditions contribute to elevated as-cast hardness [20]. The established correlation between hardness and tensile strength in HPDC alloys further supports expectations of improved mechanical effectiveness with optimized Mg additions and controlled cooling rates. However, excessive Mg and Cu enrichment during terminal solidification stages may increase susceptibility to porosity and hot tearing if inadequate feeding occurs, necessitating careful consideration in alloy and process design.

Mg additions to Al–10Si alloys promote dendritic refinement and solute redistribution. Scheil solidification simulations reveal substantial Mg accumulation in interdendritic regions with increasing solid fraction. This enhanced segregation of Mg and Cu/Si elements facilitates the formation of refined Al–Si–Mg–Cu eutectic microstructures. In scenarios characterized by swift quenching common to High-Pressure Die Casting (HPDC), the synergistic relationship between elevated cooling rates and magnesium supplementation results in a marked reduction of secondary dendrite arm spacing (SDAS). Simulations predict pronounced SDAS reduction with increasing cooling rates, with consistently finer spacings in higher-Mg alloys. This behavior follows the established $\lambda_2 \propto R^{-1/3}$ relationship (where R represents cooling rate) typical of Al–Si alloys. For instance, at low Mg levels (~0.27 wt.%), SDAS decreases from ~280–300 μm (at ~0.02°C/s) to ~10–12 μm (at 100–150°C/s), while moderate Mg additions (3.26 wt.%) reduce SDAS from ~140 μm to 8–9 μm under high cooling rates. These predictions align with Rontó and Roósz's [21] reported exponent of –1/3 for Al–Si and Al–Mg–Si systems.

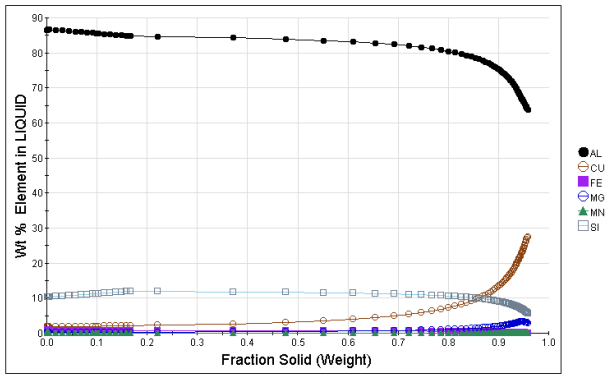

(a) Normal

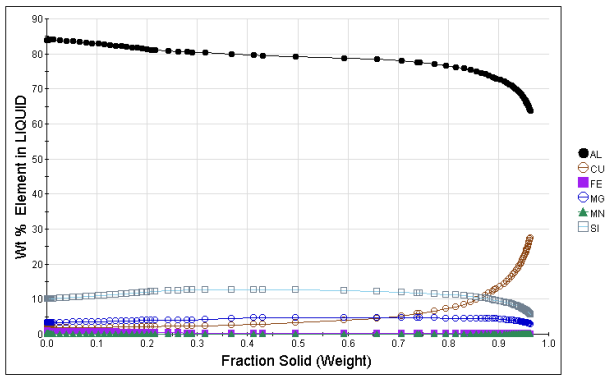

(b) Mg 3%wt

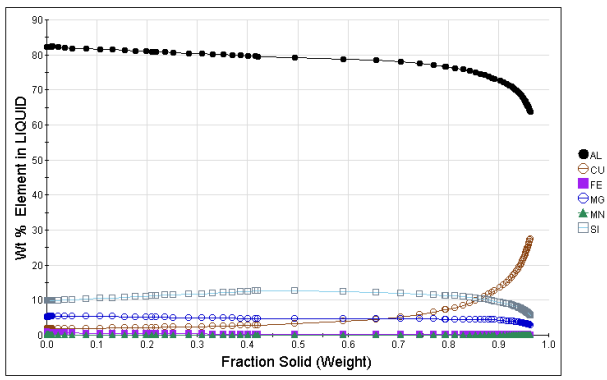

(c) Mg 5%wt

Figure 3. Liquid-phase composition evolution during solidification of Al–10Si alloys

The base Al–10Si alloy without Mg exhibits coarse α-Al dendrites and acicular silicon eutectic structures. Mg additions modify this microstructure through dendritic refinement, silicon eutectic morphological transition to coral-like structures, and significant grain size reduction (~35% decrease at 3 wt.% Mg compared to Mg-free alloys) [22]. Additionally, Mg_2Si intermetallic phases become increasingly refined and uniformly distributed with higher Mg content. Li et al. [22] reported eutectic Mg_2Si particle size reduction from ~10 μm (0.4% Mg) to ~3 μm (0.8% Mg), with further refinement at 2% Mg. This phenomenon suggests Mg additions not only increase Mg_2Si fraction but also constrain particle growth within confined interdendritic spaces [22]. Consequently, the interdendritic regions become partitioned by refined Al–Si phases, and dendritic crystals become increasingly encapsulated by residual liquid, thereby suppressing formation of coarse Mg_2Si compounds [2].

3.2 Effect of cooling rate and Mg content on mechanical properties

Figure 4 illustrates the significant influence of cooling rate on mechanical properties across all Mg addition levels, demonstrating consistent enhancement of tensile strength (blue data points), 0.2% yield strength (red data points), and hardness (black curve) with increasing cooling rates. In the baseline alloy without Mg addition (0 g), tensile strength increases from approximately 120 MPa at very low cooling rates (≈0.01°C/s) to 350-370 MPa at high cooling rates (≈100-300°C/s), while the 0.2% proof stress shows a corresponding increase from ≈65 MPa to 200-230 MPa. The addition of 15 g Mg further enhances these properties, with tensile strength ranging from ≈140 MPa (low rate) to 420-480 MPa (high rate) and 0.2% proof stress reaching 260-300 MPa under rapid cooling conditions. Although the 25 g Mg addition also demonstrates substantial improvement, its peak strength values (tensile: 390-410 MPa; proof: 240-270 MPa at high rates) are slightly lower than those achieved with 15 g Mg. These trends confirm that high cooling rates (spanning approximately 0.01 to 300°C/s) refine microstructural features and promote solute trapping, thereby enhancing strength and hardness properties [23]. The optimal mechanical effectiveness observed at intermediate Mg levels (15 g) subsequently diminishes with excessive Mg addition due to the formation of detrimental intermetallic phases.

The mechanical characteristic augmentation with escalating cooling velocities ensues from microstructural amelioration encompassing grain dimension diminution, eutectic silicon disintegration, and supersaturation of Si/Mg solutes within the aluminum matrix [24]. The modifications in microstructure bolster the alloy via dislocation blockage and a higher volumetric proportion of tiny reinforcing precipitates. Intermediate Mg additions (15 g) promote formation of Al-Mg-Si (Mg_2Si) precipitates that provide substantial precipitation strengthening, while excessive Mg additions lead to formation of hard and brittle intermetallic phases (including excess Mg_2Si and Al-Fe-Mg-Si complexes) that may compromise strength enhancement or reduce toughness [25].

Hardness and ductility assessments furnish supplementary understanding into the strength-toughness equilibrium of these alloys. Recent investigations concerning Al-Si-Mg alloys document escalating apex hardness values with augmented Mg concentration. Wenner et al. [26] documented Vickers hardness values of ≈98 HV for alloys containing ≈0.25 wt.% Mg, increasing to 119–123 HV when Mg content reached 0.45–0.60 wt.% following initial aging treatments. The tensile strength ranges reported for rapidly processed Al-Si-Mg alloys (HPDC reference) show considerable variation: Van Cauwenbergh et al. [17] reported ultimate tensile strengths of 300–450 MPa with elongations of 4–13% for AlSi10Mg in both as-built and heat-treated conditions, depending on specific thermal and processing parameters. The maximum UTS value of 428 MPa (T5 treated, 25 g Mg) observed in this study falls within the upper range of reported values for rapidly solidified/processed AlSi10Mg. The observed hardness increase at 25 g Mg (T5) corresponds with the elevated UTS values, consistent with precipitation mechanisms that hinder dislocation motion and reinforcement through refined eutectic structures and Mg_2Si dispersoids [26].

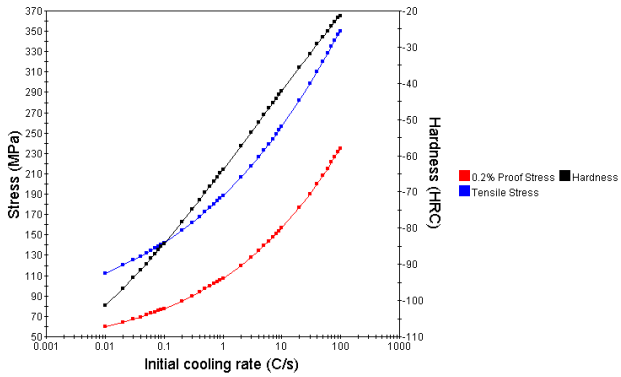

(a) Normal (Mg 0 g)

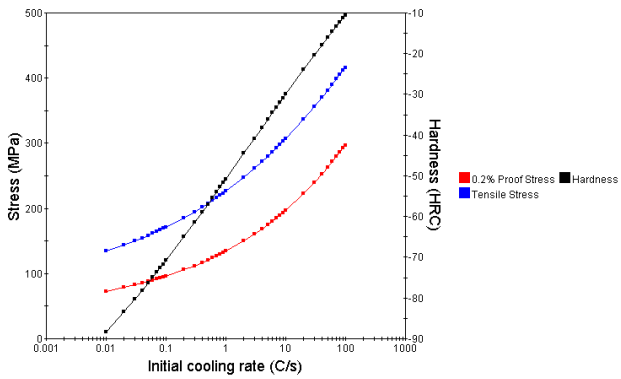

(b) Mg 15 g

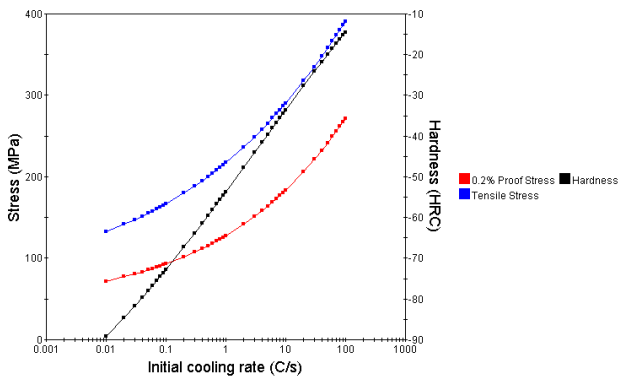

(c) Mg 25 g

Figure 4. The relationship between cooling rate and the hardness and strength qualities of the Al-10Si alloy

The examination of simulation results alongside empirical findings (Table 3) demonstrates substantial agreement. Guo et al. [15] demonstrated that rapid solidification techniques can

elevate the ultimate tensile strength of Al-Si-Mg alloys beyond 400 MPa through microstructural refinement and generation of fine precipitates, aligning with the peak values of 420–480 MPa observed at 15 g Mg addition in this study. Similarly, Shen et al. [16] reported that increasing cooling rates from approximately 10^1 to 10^2–10^3 °C/s significantly enhances tensile strength and hardness through solute trapping and eutectic silicon modification—mechanisms that correspond well with the log-linear increases in tensile strength, proof stress, and hardness observed in our data. Conversely, Shetty et al. [9] and Zhu et al. [27] note that while moderate Mg additions promote beneficial Mg_2Si precipitation strengthening, excessive Mg content (>≈1 wt.%) leads to the formation of brittle intermetallic phases that can degrade overall mechanical performance [5, 28].

Table 3. Comparison of study results

Factor	Study	Literature
UTS maximum	~420 MPa (3,26 wt% Mg + fast)	~262 MPa (water quench, no additional Mg) [29]
Hardness maximum	~18–20 HRC (baseline), ~10 HRC (at 3.26 wt%)	+130% hardness (α-Al) at water quench ~1,61 GPa [29]
Mg effect	Optimal at ~3 wt%, decreased at ~5 wt%	β-Mg_2Si increases strength, but too high Mg can be brittle [5]
Microstructure	Refinement Si & intermetals via cooling + Mg	Modification eutectic Si, undercooling +23°C [30]

This mechanistic understanding explains why the 25 g Mg addition increases hardness but yields slightly lower UTS and proof stress values compared to the 15 g Mg optimum. Quantitatively, the experimental data demonstrate that without Mg addition, tensile strength increases from ≈120 MPa to 350–370 MPa and proof stress from ≈65 MPa to 200-230 MPa as cooling rates increase from very low to high values. At 15 g Mg supplementation, these metrics ascend to 420-480 MPa (tensile) and 260-300 MPa (proof stress), whereas at 25 g Mg, the analogous metrics are 390-410 MPa (tensile) and 240-270 MPa (proof stress). These findings indicate that applying high cooling rates in combination with moderate Mg additions effectively refines microstructures while maximizing precipitation strengthening and minimizing the risk of brittle phase formation.

3.3 Effects of composition and heat treatment

The progressive addition of magnesium (0 g, 15 g, 25 g) to Al-10Si alloys produced the most significant strengthening effect following T5 heat treatment, with the maximum tensile strength of 428.42 MPa achieved at 25 g Mg addition. This result is congruent with the reports articulated by Dahle et al. [31] and Zhang et al. [32], who documented increases in ultimate tensile strength from 232 MPa to 326 MPa with elevated Mg content in Al-Si-Cu-Mg alloys, demonstrating the efficacy of Mg_2Si precipitation in enhancing alloy strength. Conversely, T6 thermal processing exhibited diminished effectiveness at moderate magnesium concentrations, possibly due to influences associated with over-aging or the obstruction of precipitation. This assessment matches the research surrounding laser powder bed fused AlSi10Mg, which reveals that T6 treatment leads to a hardness drop in relation to the as-fabricated state [33]. While more complex T6-type heat treatments can provide better strength-ductility balance, they generally do not maximize strength to the same extent as T5 treatment when applied to already refined microstructures [27].

The enhanced tensile strength in high-Mg compositions (25 g, ≈ 5.26 wt.%) can be explained through microstructural analysis. Under die casting of high-pressure (HPDC) conditions employing cooling rates of 60-125 $K \cdot s^{-1}$, refined secondary dendrite arm spacing (SDAS) creates numerous favorable sites for β-Mg_2Si precipitation. Van Cauwenbergh et al. [17] demonstrated that the distribution of magnesium and silicon within interdendritic regions during rapid solidification promotes the formation of fine precipitates during subsequent aging, representing the fundamental strengthening mechanism. Thus, the observed maximum UTS at 25 g Mg with T5 treatment aligns well with this precipitation-based reinforcement mechanism. Nevertheless, these advantages must be weighed against augmented hazards of porosity and thermal fracturing, as evidenced in High-Pressure Die Casting studies conducted by Dahle et al. [31], where elevated magnesium content impaired mold filling capability without appropriate feeding system design.

Simulation findings elucidate a uniform reduction in secondary dendrite arm spacing (SDAS) with escalating cooling rates, with systematically diminished values noted at elevated Mg concentrations (Figure 5). In low-Mg alloys (~0.27 wt.%), Secondary Dendrite Arm Spacing (SDAS) diminished from roughly 280-300 μm at ~0.02 $°C \cdot s^{-1}$ to 10-12 μm at 100-150 $°C \cdot s^{-1}$. A similar trend occurred in medium-Mg alloys (~3.26 wt.%), where SDAS reduced from 140 μm to 8-9 μm, and high-Mg alloys (~5.26 wt.%) exhibited even finer spacing, decreasing from 105 μm to 6-7 μm. The parallel nature of these curves indicates that while cooling rate predominantly governs dendritic refinement, Mg addition further reduces SDAS values across all cooling conditions. This relationship follows the established empirical model where SDAS is inversely proportional to the cube root of cooling rate ($\lambda_2 \propto R^{-1/3}$) [34, 35].

These results corroborate the findings of Rontó and RoÓlSz [36], who demonstrated that the -1/3 exponent generally applies to Al-Si and Al-Mg-Si alloys, with proportionality constants varying according to dissolved element content. Quantitative correlations from studies on A356 alloys (Al-7Si-0.3Mg) yielded the equation $\lambda_2 \approx 40.7R^{-1/3}$, producing SDAS values of ~40.7 μm at $1°C \cdot s^{-1}$, ~18.9 μm at $10°C \cdot s^{-1}$, and ~8.8 μm at $100°C \cdot s^{-1}$. This range confirms that in HPDC processes typically operating at 10-100$°C \cdot s^{-1}$, the resulting SDAS values fall within the 9-19 μm range [16, 37].

Zhang et al. [38] reported that regions experiencing low

cooling rates (<0.3°C·s⁻¹) developed SDAS values >45 μm, significantly reducing material fatigue resistance. Conversely, HPDC conditions producing SDAS ≤20 μm contribute to enhanced strength, toughness, and response to T5 and T6 heat treatments. These studies jointly substantiate the finding that regulated cooling velocities alongside Mg additions work hand in hand to optimize dendritic microstructure, thereby enhancing the mechanical features of Al-Si-Mg alloys.

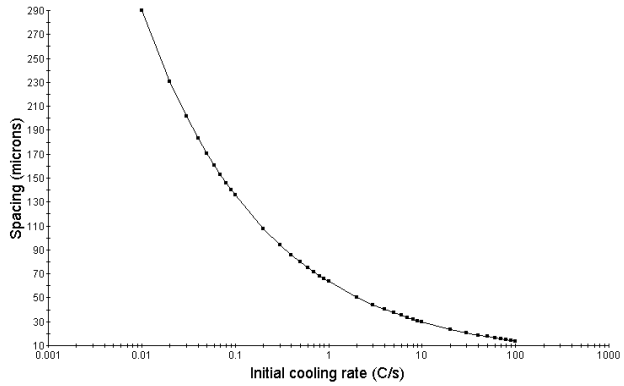

a) Normal

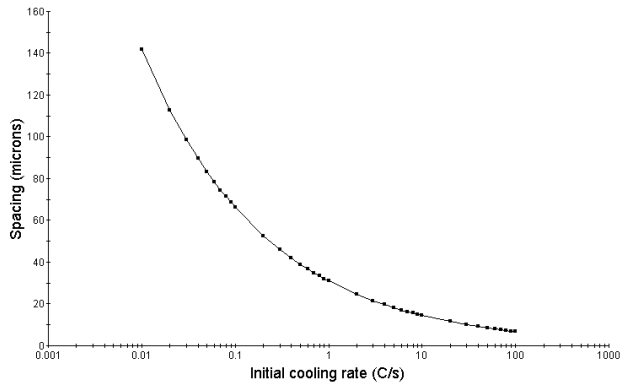

b) Mg 15 g

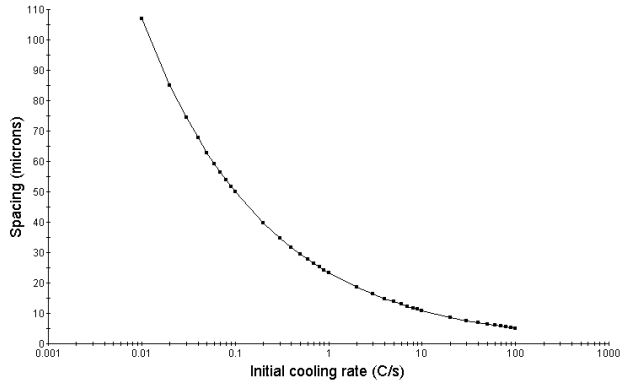

c) Mg 25 g

Figure 5. Secondary dendrite arm spacing versus cooling rate

4. CONCLUSIONS

Introducing magnesium to Al-10Si alloys aids in the formation of β-Mg_2Si precipitates during the aging phase, consequently boosting hardness and ultimate tensile strength (UTS). Under rapid solidification conditions characteristic of high-pressure die casting (HPDC), moderate Mg additions (~3 wt.%, equivalent to 15 g) yielded the optimal strength-ductility balance. In contrast, higher Mg concentrations (~5.25 wt.%, 25 g) increased hardness but reduced both UTS and ductility due to the formation of coarse intermetallic compounds and an elevated risk of porosity and interdendritic defects. The rapid cooling rates inherent to HPDC significantly reduced secondary dendrite arm spacing (SDAS), and when combined with Mg_2Si precipitation during T5 aging, produced synergistic strengthening effects. To enhance mechanical properties, a unified adjustment in composition elements alongside treatment parameters, including cooling speeds and aging techniques, is essential.

JMatPro simulations employing Scheil solidification and precipitation modeling demonstrated qualitative agreement with experimental trends, proving valuable for mapping composition-process parameter relationships. Nevertheless, their numerical precision is substantially contingent upon accurate cooling rate distribution inputs and necessitates corroboration against more extensive experimental data. For practical HPDC applications, we recommend employing moderate Mg additions (~3 wt.%) coupled with optimized feeding and gating systems to minimize porosity, combined with T5 aging to maximize precipitation strengthening.

This investigation's constraints encompass the limited quantity of experimental replications and the presumption of standard cooling velocities in simulations. Future research should incorporate: 1) A minimum of 3-5 replicates per experimental condition, 2) Detailed defect characterization through SEM analysis of intermetallic phases and porosity distribution, and 3) In-situ cooling rate measurements to enhance simulation boundary conditions.

ACKNOWLEDGMENT

The authors genuinely acknowledge the essential support and facilitation provided by the Director of the Research and Community Service Institute (LPPM) at Universitas Cenderawasih and by the Division of Mechanical Engineering throughout the duration of this study.

REFERENCES

[1] Tian, N., Wang, G., Zhou, Y., Liu, C., Liu, K., Zhao, G., Zuo, L. (2021). Formation of Phases and Microstructures in Al-8Si alloys with different Mg content. Materials, 14(4): 762. https://doi.org/10.3390/ma14040762

[2] Gandolfi, M., Xavier, M.G.C., Gomes, L.F., Reyes, R.A.V., Garcia, A., Spinelli, J.E. (2021). Relationship between microstructure evolution and tensile properties of AlSi10Mg alloys with varying Mg content and solidification cooling rates. Metals, 11(7): 1019. https://doi.org/10.3390/met11071019

[3] Merayo Fernández, D., Rodríguez-Prieto, A., Camacho, A.M. (2020). Prediction of the bilinear stress-strain curve of aluminum alloys using artificial intelligence and big data. Metals, 10(7): 904. https://doi.org/10.3390/met10070904

[4] Annamalai, S., Periyakgoundar, S., Gunasekaran, S. (2019). Magnesium alloys: A review of applications. Materials & Technologies/Materiali in Tehnologije, 53(6): 881-890. https://doi.org/10.17222/mit.2019.065

[5] Beder, M., Akçay, S.B., Varol, T., Çuvalcı, H. (2024). The effect of heat treatment on the mechanical properties and oxidation resistance of AlSi10Mg alloy. Arabian

Journal for Science and Engineering, 49(11): 15335-15346. https://doi.org/10.1007/s13369-024-08971-1
[6] Ji, K., Li, L., Liang, J., Li, C., Zhao, X., Han, Q., Zhang, Y. (2024). Effect of strontium modification on microstructure and mechanical property Al12SiCuMgNi alloy in squeeze casting. Journal of Physics: Conference Series, 2785(1): 012153. https://doi.org/10.1088/1742-6596/2785/1/012153
[7] Mathew, J., Williams, M.A., Srirangam, P. (2021). X-ray computed tomography studies on porosity distribution in vacuum induction cast Al-7Si Alloys. JOM, 73(12): 3866-3872. https://doi.org/10.1007/s11837-021-04944-z
[8] Jin, B.R., Ha, D.W., Jeong, C.Y. (2019). Effect of solution treatment on the hardness and tensile properties of Al–Mg–Si alloys for automotive chassis. Materials Transactions, 60(5): 815-823. https://doi.org/10.2320/matertrans.M2018368
[9] Shetty, A., Bhat, T., Sharma, S., Hegde, A., K, N., Prabhu, R., Anne, G. (2024). Effects of magnesium content and age hardening parameters on the hardness and ultimate tensile strength of SiC-reinforced Al-Si-Mg composites. Journal of Composites Science, 9(1): 5. https://doi.org/10.3390/jcs9010005
[10] Chinababu, M., Naga Krishna, N., Sivaprasad, K., Prashanth, K.G., Bhaskara Rao, E. (2021). Evolution of microstructure and mechanical properties of LM25–HEA composite processed through stir casting with a bottom pouring system. Materials, 15(1): 230. https://doi.org/10.3390/ma15010230
[11] Palai, D., Siva Prasad, P., Satpathy, B., Das, S., Das, K. (2023). Development of Zn-2Cu-x Mn/Mg alloys for orthopedic applications: Mechanical performance to in vitro degradation under different physiological environments. ACS Biomaterials Science & Engineering, 9(11): 6058-6083. https://doi.org/10.1021/acsbiomaterials.3c00641
[12] Guan, Z., Linsley, C.S., Pan, S., Yao, G., Wu, B.M., Levi, D.S., Li, X. (2021). Zn–Mg–WC nanocomposites for bioresorbable cardiovascular stents: Microstructure, mechanical properties, fatigue, shelf life, and corrosion. ACS Biomaterials Science & Engineering, 8(1): 328-339. https://doi.org/10.1021/acsbiomaterials.1c01358
[13] Breton, F., Fourmann, J. (2023). Performance and fundamental differences between rheocast and High-Pressure Vacuum Die Cast Al-Si-Mg alloys. Solid State Phenomena, 348: 75-82. https://doi.org/10.4028/p-p5sK4z
[14] Martinez, F., Junior, C.D.S., Leal, J., Silva, A., Gouveia, G., Spinelli, J. (2023). Effects of Sc addition and direct aging treatment on microstructure and hardness of AlSi10Mg alloy. Advanced Engineering Materials, 25(19): 2300596. https://doi.org/10.1002/adem.202300596
[15] Guo, M., Sun, M., Huang, J., Pang, S. (2022). A comparative study on the microstructures and mechanical properties of Al-10Si-0.5 Mg alloys prepared under different conditions. Metals, 12(1): 142. https://doi.org/10.3390/met12010142
[16] Shen, X., Liu, S., Wang, X., Cui, C., Gong, P., Zhao, L., Li, Z. (2022). Effect of cooling rate on the microstructure evolution and mechanical properties of Iron-Rich Al–Si alloy. Materials, 15(2): 411. https://doi.org/10.3390/ma15020411
[17] Van Cauwenbergh, P., Samaee, V., Thijs, L., Nejezchlebová, J., Sedlak, P., Iveković, A., Vanmeensel, K. (2021). Unravelling the multi-scale structure–property relationship of laser powder bed fusion processed and heat-treated AlSi10Mg. Scientific Reports, 11(1): 6423. https://doi.org/10.1038/s41598-021-85047-2
[18] Hennum, E., Marthinsen, K., Tundal, U.H. (2024). Effect of microstructure on the precipitation of β-Mg2Si during cooling after homogenisation of Al-Mg-Si alloys. Metals, 14(2): 215. https://doi.org/10.3390/met14020215
[19] Ali, R., Al-Zubaidy, B. (2024). Investigation of the effect of aluminium addition on the additively manufactured SS309L alloy. Annales de Chimie - Science des Matériaux, 48(2): 177-186. https://doi.org/10.18280/acsm.480204
[20] Žbontar, M., Petrič, M., Mrvar, P. (2021). The influence of cooling rate on microstructure and mechanical properties of AlSi9Cu3. Metals, 11(2): 186. https://doi.org/10.3390/met11020186
[21] Rontó, V., Roósz, A. (2002). Numerical simulation of dendrite arm coarsening in the case of ternary Al alloys. Materials Science Forum, 414: 483-490. https://doi.org/10.4028/www.scientific.net/MSF.414-415.483
[22] Li, Q., Qiu, F., Dong, B.X., Yang, H.Y., Shu, S.L., Zha, M., Jiang, Q.C. (2020). Investigation of the influences of ternary Mg addition on the solidification microstructure and mechanical properties of as-cast Al–10Si alloys. Materials Science and Engineering: A, 798: 140247. https://doi.org/10.1016/j.msea.2020.140247
[23] Mauduit, A., Salesse, L., Bachelard, N., Gransac, H. (2025). A study of nanostructured 7034 aluminium alloy: Relationship between microstructure and mechanical properties. Annales de Chimie - Science des Matériaux, 49(3): 219-233. https://doi.org/10.18280/acsm.490301
[24] Tambing, E., Agustinus, Pagasis, T., Ranteallo, O.T., Mangallo, D. Joni. (2025). Effects of flowing water cooling on the quenching process of AISI 1045 steel: Influence on tensile strength, hardness, and microstructure. Revue des Composites et des Matériaux Avancés-Journal of Composite and Advanced Materials, 35(1): 117-126. https://doi.org/10.18280/rcma.350114
[25] Hao, J., Yu, B., Bian, J., Chen, B., Wu, H., Li, W., Li, R. (2021). Calculation based on the formation of Mg2Si and its effect on the microstructure and properties of Al–Si alloys. Materials, 14(21): 6537. https://doi.org/10.3390/ma14216537
[26] Wenner, S., Hatzoglou, C., Mørtsell, E.A., Åsholt, P. (2023). Clustering and precipitation during early-stage artificial aging of Al–Si–Mg (–Cu) foundry alloys. Metals, 13(3): 557. https://doi.org/10.3390/met13030557
[27] Zhu, X., Yang, H., Dong, X., Ji, S. (2019). The effects of varying Mg and Si levels on the microstructural inhomogeneity and eutectic Mg2Si morphology in die-cast Al–Mg–Si alloys. Journal of Materials Science, 54(7): 5773-5787. https://doi.org/10.1007/s10853-018-03198-6
[28] Dang, B., Zhang, X., Chen, Y.Z., Chen, C.X., Wang, H.T., Liu, F. (2016). Breaking through the strength-ductility trade-off dilemma in an Al-Si-based casting alloy. Scientific Reports, 6(1): 30874. https://doi.org/10.1038/srep30874

[29] Lee, E., Mishra, B. (2017). Effect of solidification cooling rate on mechanical properties and microstructure of Al-Si-Mn-Mg alloy. Materials Transactions, 58(11): 1624-1627. https://doi.org/10.2320/matertrans.M2017170

[30] Aguilera-Luna, I., Castro-Román, M.J., Escobedo-Bocardo, J.C., García-Pastor, F.A., Herrera-Trejo, M. (2014). Effect of cooling rate and Mg content on the Al–Si eutectic for Al–Si–Cu–Mg alloys. Materials Characterization, 95: 211-218. https://doi.org/10.1016/j.matchar.2014.06.009

[31] Dahle, A.K., Nogita, K., McDonald, S.D., Dinnis, C., Lu, L. (2005). Eutectic modification and microstructure development in Al–Si alloys. Materials Science and Engineering: A, 413: 243-248. https://doi.org/10.1016/j.msea.2005.09.055

[32] Zhang, P., Li, Z., Liu, B., Ding, W., Peng, L. (2016). Improved tensile properties of a new aluminum alloy for high pressure die casting. Materials Science and Engineering: A, 651: 376-390. https://doi.org/10.1016/j.msea.2015.10.127

[33] Yu, X., Wang, L. (2018). T6 heat-treated AlSi10Mg alloys additive-manufactured by selective laser melting. Procedia Manufacturing, 15: 1701-1707. https://doi.org/10.1016/j.promfg.2018.07.265

[34] Zhang, Q., Fang, H., Xue, H., Pan, S., Rettenmayr, M., Zhu, M. (2017). Interaction of local solidification and remelting during dendrite coarsening-modeling and comparison with experiments. Scientific Reports, 7(1): 17809. https://doi.org/10.1038/s41598-017-17857-2

[35] Kraft, T., Chang, Y.A. (1998). Discussion of "Effect of dendrite arm coarsening on microsegregation." Metallurgical and Materials Transactions A, 29(9): 2447–2449. https://doi.org/10.1007/s11661-998-0120-3

[36] Ronté, V., RoÓlSz, A. (2001). The effect of cooling rate and composition on the secondary dendrite arm spacing during solidification. Part I: Al-Cu-Si alloys. International Journal of Cast Metals Research, 13(6): 337-342. https://doi.org/10.1080/13640461.2001.11819415

[37] Shabani, M.O., Mazahery, A. (2011). Prediction of mechanical properties of cast A356 alloy as a function of microstructure and cooling rate. Archives of Metallurgy and Materials, 56(3): 671-675. https://doi.org/10.2478/v10172-011-0073-1

[38] Zhang, Chen, Poirier. (2000). Effect of solidification cooling rate on the fatigue life of A356.2-T6 cast aluminium alloy. Fatigue & Fracture of Engineering Materials & Structures, 23(5): 417-423. https://doi.org/10.1046/j.1460-2695.2000.00299.x